THE ASTROPHYSICAL JOURNAL, 652:L21–L24, 2006 November 20
© 2006. The American Astronomical Society. All rights reserved. Printed in U.S.A.

A LARGE MASS OF H_2 IN THE BRIGHTEST CLUSTER GALAXY IN ZWICKY 3146

E. EGAMI,[1] G. H. RIEKE,[1] D. FADDA,[2] AND D. C. HINES[3]

Received 2006 August 4; accepted 2006 October 5; published 2006 October 30

ABSTRACT

We present the *Spitzer*/IRS mid-infrared spectrum of the infrared-luminous ($L_{\rm IR} = 4 \times 10^{11}\ L_\odot$) brightest cluster galaxy (BCG) in the X-ray–luminous cluster Zwicky 3146 (Z3146; $z = 0.29$). The spectrum shows strong aromatic emission features, indicating that the dominant source of the infrared luminosity is star formation. The most striking feature of the spectrum, however, is the exceptionally strong molecular hydrogen (H_2) emission lines, which seem to be shock-excited. The line luminosities and inferred warm H_2 gas mass ($\sim 10^{10}\ M_\odot$) are 6 times larger than those of NGC 6240, the most H_2-luminous galaxy at $z \lesssim 0.05$. Together with the large amount of cold H_2 detected previously ($\sim 10^{11}\ M_\odot$), this indicates that the Z3146 BCG contains disproportionately large amounts of both warm and cold H_2 gas for its infrared luminosity, which may be related to the intracluster gas cooling process in the cluster core.

Subject headings: cooling flows — galaxies: active — galaxies: clusters: general — galaxies: elliptical and lenticular, cD — infrared: galaxies

1. INTRODUCTION

Zwicky 3146 (Z3146)[4] is an X-ray–luminous cluster of galaxies at a redshift of 0.29. Its soft (0.1–2.4 keV) X-ray luminosity[5] of 2×10^{45} ergs s^{-1} (Ebeling et al. 1998; Böhringer et al. 2000) is one of the largest known, and based on the *ROSAT* data, Z3146 was thought to exhibit one of the most massive cluster cooling flows (Edge et al. 1994). Our analysis of *Chandra* data confirms that the gas cooling rate is indeed large, with an estimated mass deposition rate of $\sim 300\ M_\odot$ yr^{-1} within a 50 kpc radius from the cluster center (Egami et al. 2006).

The brightest cluster galaxy (BCG) is exceptionally active, showing a blue continuum and luminous nebular emission lines (Allen et al. 1992; Hicks & Mushotzky 2005) and an infrared luminosity of $4 \times 10^{11}\ L_\odot$ (Egami et al. 2006). The mid-infrared spectral energy distribution suggests that the source of the large infrared luminosity is star formation at a rate of $\sim 70\ M_\odot$ yr^{-1}, broadly consistent with the mass deposition rate mentioned above. This may indicate that the active star formation is caused by cooling cluster gas accreting onto the BCG, i.e., the cooling flow (Cowie & Binney 1977; Fabian & Nulsen 1977). At the same time, the BCG seems to contain a radio active galactic nucleus (AGN) that may contribute to its luminosity (Egami et al. 2006).

To investigate the mid-infrared spectral properties in detail, we have observed the BCG in Z3146 using the Infrared Spectrograph (IRS; Houck et al. 2004) on board the *Spitzer Space Telescope* (Werner et al. 2004).

2. OBSERVATIONS AND DATA REDUCTION

The IRS spectra of the BCG in Z3146 covering 5–38 μm were taken in the staring mode with the two low-resolution modules, Short-Low (SL; $\Delta\lambda = 5.2$–$14.5\ \mu$m) and Long-Low (LL; $\Delta\lambda = 14.0$–$38.0\ \mu$m), with a resolving power of $R \sim 64$–128. The SL spectra were taken for eight cycles of 60 s ramp durations for both the second (SL2: 5.2–8.7 μm) and first (SL1: 7.4–14.5 μm) orders, while the LL spectra were taken for eight cycles of 120 s ramp durations for the second order (LL2: 14.0–21.3 μm) and six cycles for the first order (LL1: 19.5–38.0 μm). The resultant integration times are 960 s (SL1 and SL2), 1920 s (LL2), and 1440 s (LL1) after co-adding the spectra taken at the two nod positions. The slit width is 3.″7 for the SL and 10.″7 for the LL module.

Starting with the reduced and co-added two-dimensional spectral image at each nod position, we performed sky subtraction in two passes, first by taking the difference between the two nod positions (spectral images targeting different orders were paired to avoid both the positive and negative spectra falling in the same order) and second by fitting and subtracting a linear fit to the background along each row in the cross-dispersed direction (only fitting the pixels well away from the source spectrum). Then, pixels with an abnormal signal near the source spectrum were manually masked out from the subsequent processing. From the background-subtracted and cleaned spectral images, the source spectrum was extracted at each nod position using the program SPICE[6] with extraction apertures reduced to 75% of the default widths. All the spectra were combined by resampling them with a uniform resolving power of 130 over the whole wavelength range. Finally, the combined spectrum was multiplied by 1.4 to match the IRAC (Infrared Array Camera) 8.0 μm and MIPS (Multiband Image Photometer for *Spitzer*) 24 μm photometry.

3. RESULTS

The final combined IRS spectrum of the BCG in Z3146 is shown in Figure 1. The measured line fluxes and rest-frame equivalent widths are listed in Table 1. Along the spatial direction, the lines and continuum are unresolved (FWHM $\sim$ 2 pixels), which sets an upper limit of 3.″6 in SL and 10.″2 in LL on the size of the mid-infrared–emitting region. This is consistent with the fact that the Z3146 BCG is barely resolved at 8 μm with a spatial resolution of 2″ (Egami et al. 2006).

Strong aromatic (polycyclic aromatic hydrocarbon, "PAH")

[1] Steward Observatory, University of Arizona, 933 North Cherry Avenue, Tucson, AZ 85721.

[2] NASA *Herschel* Science Center, California Institute of Technology, MC 100-22, 770 South Wilson Avenue, Pasadena, CA 91125.

[3] Space Science Institute, 4750 Walnut Street, Suite 205, Boulder, CO 80301.

[4] The NASA/IPAC Extragalactic Database (NED) name of this cluster is ZwCl 1021.0+0426.

[5] Throughout the Letter, we adopt the cosmological parameters of $\Omega_M = 0.3$, $\Omega_\Lambda = 0.7$, and $H_0 = 70$ km s^{-1}.

[6] See http://ssc.spitzer.caltech.edu/postbcd/spice.html.

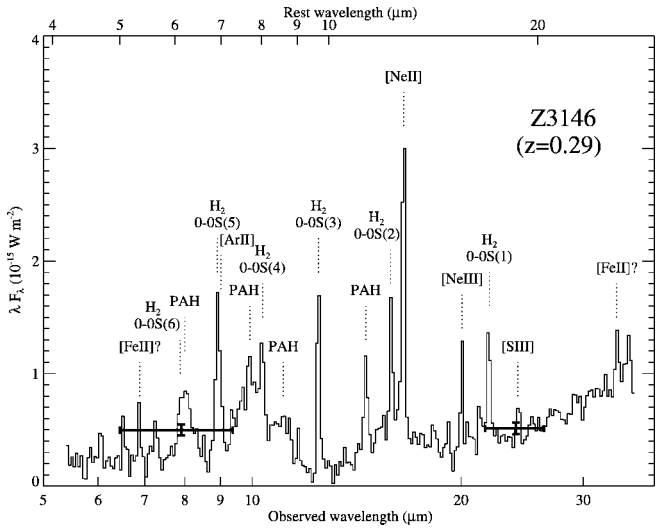

FIG. 1.—Combined IRS spectrum of the BCG in Z3146. The two points with error bars show the IRAC 8.0 μm and MIPS 24 μm photometry from Egami et al. (2006). The IRS spectrum has been scaled ($\times$ 1.4) to match these photometry points when the spectrum is integrated over the corresponding passbands.

emission features are detected at 6.2, 7.7, 8.6, and 11.3 μm. These features indicate that the mid-infrared (and therefore presumably the far-infrared) luminosity of this galaxy has a significant component of active star formation.

The spectrum also shows exceptionally strong emission lines from molecular hydrogen (H_2). We have securely detected the 0–0 $S(1)$, $S(2)$, $S(3)$, $S(4)$, and $S(5)$ pure rotational lines. Although the 0–0 $S(0)$ line is within the observed wavelength range ($\lambda_{obs} = 36.4$ μm), the noise in the LL1 band increases dramatically beyond 35 μm, preventing us from setting a meaningful upper limit on the line flux. The 0–0 $S(6)$ line is blended with the bright 6.2 μm PAH feature nearby.

A few atomic fine-structure emission lines are also detected in the spectrum, such as [Ne II] 12.8 μm and [Ne III] 15.5 μm. The [S III] 18.7 μm line is possibly detected as well, but because of the low signal-to-noise ratio, we treat it as a nondetection here. Also, no high-ionization line (e.g., [Ne V] 15.6 μm) is seen. The small [Ne III]/[Ne II] line ratio of 0.2 is typical of a starburst galaxy (Thornley et al. 2000), although we cannot rule out a significant contribution to these neon lines from a shock-excited gas, as discussed below.

There are possible detections of the [Fe II] lines at 5.3 and 26.0 μm. However, a longer integration time is needed to confirm the reality of these lines.

4. DISCUSSION

4.1. *PAH Features*

In terms of the strength of the 6.2 μm PAH feature, the Z3146 BCG appears to be a typical starburst-dominated infrared-luminous galaxy. The rest-frame equivalent width of the feature (0.67 μm) as well as the ratio of its luminosity to the total infrared luminosity (5×10^{-3}) are both within the range found for starburst galaxies, $\sim$0.6 $\pm$ 0.1 μm for the former (Weedman et al. 2005) and $(6.3 \pm 3.2) \times 10^{-3}$ for the latter (Peeters et al. 2004). Given the absence of any AGN-related features in the spectrum, the AGN contribution to the infrared luminosity is likely to be small.

TABLE 1
Z3146 BCG LINE FLUXES

λ_{rest} (μm)	Line/Feature	Flux (10^{-17} W m^{-2})	EW_{rest} (μm)
6.2	PAH	3.0 $\pm$ 0.2	0.67 $\pm$ 0.05
6.9	H_2 0–0 $S(5)$	2.1 $\pm$ 0.1	0.49 $\pm$0 .02
6.99	[Ar II][a]	$\sim$0.6	$\sim$0.15
7.7	PAH	6.9 $\pm$ 0.2	1.72 $\pm$ 0.06
8.0	H_2 0–0 $S(4)$	0.8 $\pm$ 0.1	0.19 $\pm$ 0.02
8.6	PAH	1.2 $\pm$ 0.2	0.31 $\pm$ 0.04
9.7	H_2 0–0 $S(3)$	2.3 $\pm$ 0.1	1.72 $\pm$ 0.05
11.3	PAH	1.3 $\pm$ 0.1	0.47 $\pm$ 0.07
12.3	H_2 0–0 $S(2)$	1.2 $\pm$ 0.1	0.26 $\pm$ 0.02
12.8	[Ne II]	4.2 $\pm$ 0.1	1.34 $\pm$ 0.03
15.6	[Ne III]	0.8 $\pm$ 0.1	0.30 $\pm$ 0.04
17.0	H_2 0–0 $S(1)$	1.4 $\pm$ 0.1	0.55 $\pm$ 0.04
18.7	[S III]	<0.4	<0.2

[a] The [Ar II] 6.99 μm line was not detected directly, but its presence was set to the maximum level consistent with the $S(5)$ line shape.

4.2. *Molecular Hydrogen Lines*

The most striking feature of the spectrum is the exceptionally strong emission lines from molecular hydrogen. The luminosities of the pure rotational lines are on average 6.3 times larger than those of NGC 6240, the most H_2-luminous galaxy at $z \lesssim 0.05$.

The H_2 line strengths are even more remarkable when compared with the infrared luminosity of this BCG. Figure 2*a* plots the line luminosity of the H_2 0–0 $S(1)$ emission line against the infrared luminosity of various galaxies. The H_2 0–0 $S(1)$/infrared luminosity ratio of this BCG is extreme (0.25%), almost an order of magnitude larger than the ratio for NGC 6240 (0.03%), and a factor of 50 above the trend line for the other galaxies (0.005%).

Figure 3 shows the H_2 level population in the Z3146 BCG. For comparison, the level population in NGC 6240 is overplotted after being scaled by a factor of 6.3. The level populations are quite similar in shape between the two galaxies in the lowest energy states ($v = 0$, $J = 3$–7). These lowest energy states are almost always thermalized (i.e., collisionally excited), and therefore the similarity suggests that although the

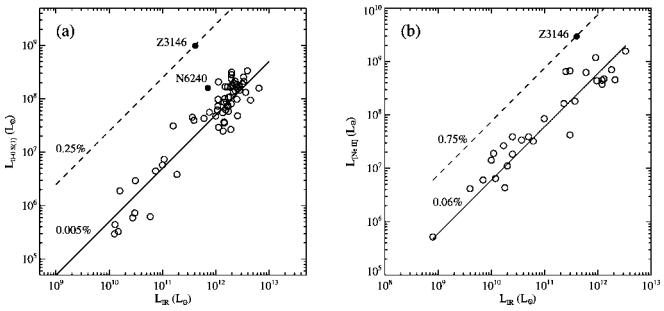

FIG. 2.—(*a*) H_2 0–0 $S(1)$ 17 μm line luminosity vs. infrared luminosity (L_{IR}). The solid and dashed lines correspond to $L_{0\text{–}0\ S(1)} = 0.005\%$ and 0.25% of L_{IR}, respectively. The H_2 line luminosities were taken from Armus et al. (2006; NGC 6240), Rigopoulou et al. (2002), and Higdon et al. (2006). Note that the H_2 luminosity correlates with the infrared luminosity, so the sample studied by Higdon et al. (2006), which extends beyond a redshift of 0.1 and therefore includes more infrared-luminous galaxies, contains galaxies more H_2-luminous than NGC 6240. (*b*) [Ne II] 12.8 μm line luminosity vs. L_{IR}. The solid and dashed lines correspond to $L_{[Ne\ II]} = 0.06\%$ and 0.75% of L_{IR}, respectively. The [Ne II] line luminosities were taken from Genzel et al. (1998), while the infrared luminosities were taken from Sanders et al. (2003).

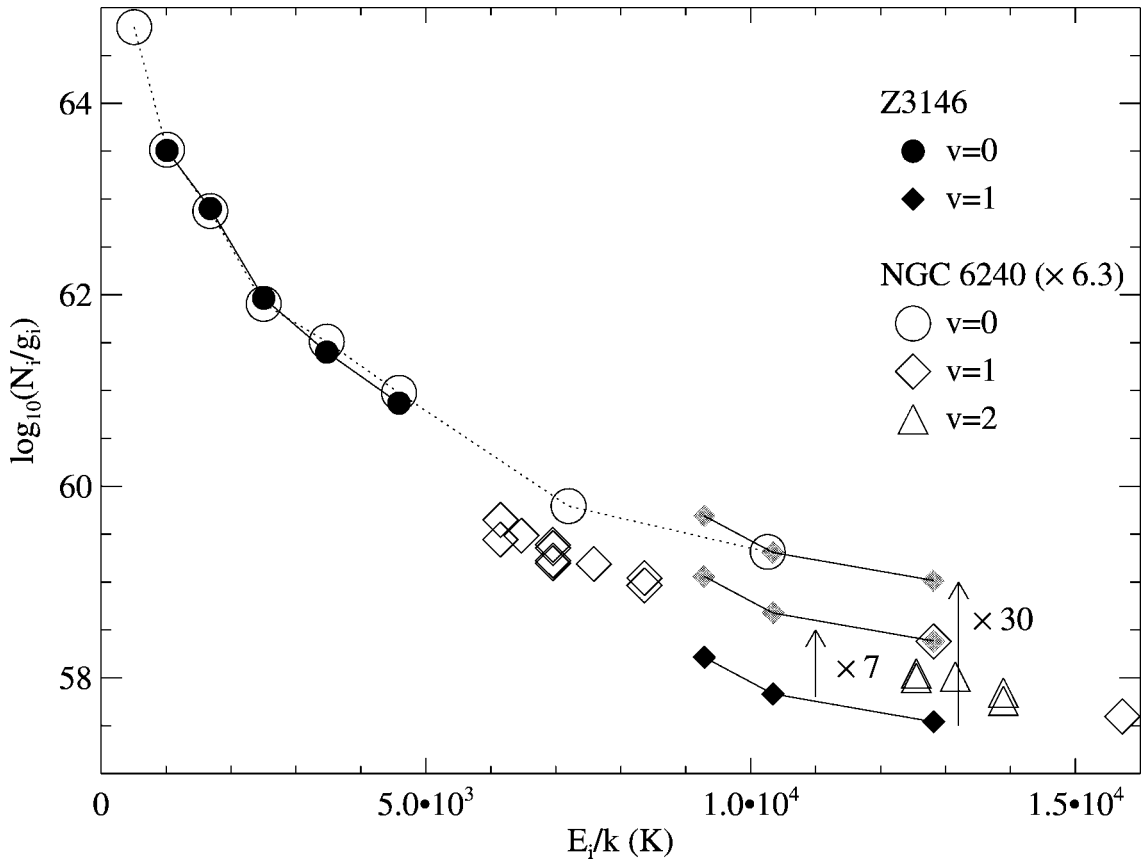

FIG. 3.—H_2 excitation diagram showing the level population of warm H_2 in the Z3146 BCG. The level population in the ground vibrational state ($v = 0$) is based on our observation, while the $v = 1$ level population was derived from the data by Edge et al. (2002). The *X*-axis is the H_2 energy level expressed in temperature (E_i is the energy level of the *i*th state; *k* is the Boltzmann constant). In the *Y*-axis, N_i refers to the *total* number of H_2 in the *i*th energy state, while g_i is the statistical weight of that state (ortho-para ratio was set to 3 : 1). Assuming that the H_2 lines are optically thin, N_i was calculated as $N_i = L_i/(A_i h\nu_i)$, where L_i is the observed line luminosity, A_i is the Einstein coefficient for that transition, h is the Planck constant, and ν_i is the frequency of the line. In comparison, the H_2 level population of NGC 6240 is also shown based on the published data (van der Werf 1996; Sugai et al. 1997; Lutz et al. 2003; Armus et al. 2006). The data from Sugai et al. (1997) were plotted by assuming that the 1–0 *S*(1) line flux agrees with that of van der Werf (1996). No other scaling was applied. The solid line connects the $v = 0$ and 1 states in the Z3146 BCG, while the dotted line connects the $v = 0$ states in NGC 6240.

total mass of warm H_2 differs between the two galaxies, the fractional H_2 mass distribution as a function of temperature is similar up to a gas temperature of ~1000 K [i.e., the H_2 excitation temperature derived for the $v = 0$, $J = 6$ and 7 states using the 0–0 *S*(4) and *S*(5) lines].

Assuming that this similarity of the level population extends down to the $v = 0$, $J = 2$ state, from which the 0–0 *S*(0) line originates, we estimate the total warm H_2 mass in the Z3146 BCG to be $\sim 10^{10}\ M_\odot$, i.e., 6.3 times larger than that of NGC 6240 ($1.6 \times 10^9\ M_\odot$ by Armus et al. 2006). This mass is dominated by the ~160 K component, a temperature derived from the 0–0 *S*(0)/0–0 *S*(1) line ratio measured for NGC 6240. The cold H_2 mass derived from the CO observation is also large, $\sim 10^{11}\ M_\odot$ (Edge & Frayer 2003), but the fraction of warm H_2 mass is high, ~10%, similar to the 15% fraction found in NGC 6240 (Armus et al. 2006).

Figure 3 also shows that the H_2 level population of the Z3146 BCG in the $v = 1$ vibrational state is highly suppressed (by a factor of 30) with respect to that in the $v = 0$ state when the NGC 6240 $v = 0$ level population is used as a template. Although part of this suppression is due to the slit loss with the near-infrared spectroscopy as well as internal dust extinction, these effects, even when combined, are unlikely to be sufficient. For example, the size of the mid-infrared–emitting region is 2″ at most, as already mentioned, so the 1.″5 slit used to measure the $v = 1$–0 near-infrared H_2 lines (Edge et al. 2002) should capture most of the total line fluxes. Also, in this BCG, the extinction derived from the Balmer decrement is $A_V = 0.6$ mag (Crawford et al. 1999), and when corrected for this amount, the Hα-derived star formation rate agrees well with the infrared-derived star formation rate (Egami et al. 2006), suggesting that the extinction cannot be much larger. In fact, near-/mid-infrared H_2 emission lines are known to show little extinction in infrared-luminous galaxies (Goldader et al. 1997; Higdon et al. 2006).

This suppression of the $v = 1$ state suggests that the $v = 1$ level population in the Z3146 BCG is subthermal, as is the case with NGC 6240 (Egami 1998; Lutz et al. 2003). Although the cause of such a subthermal level population is not clear, one possibility is that the H_2 molecules are excited by a continuous (i.e., C-type) shock, which can produce subthermal level populations in the low vibrational states (e.g., Kaufman & Neufeld 1996; Le Bourlot et al. 2002). Note that alternative excitation mechanisms such as a jump (J-type) shock or far-UV radiation would produce a $v = 1$ level population at or above the thermal level with respect to the $v = 0$ state (e.g., Burton 1992). Figure 3 shows that only a factor of ~7 scaling is required to bring up the $v = 1$ level population in the Z3146 BCG to that of NGC 6240. This correction factor is much easier to account for than the factor of 30 mentioned above, which

would be required if the $v = 1$ state is thermalized. Shock excitation is also consistent with the previous near-infrared spectroscopic studies of nearby cooling flow cluster BCGs (e.g., Jaffe et al. 2001; Wilman et al. 2002).

4.3. *Atomic Fine-Structure Lines*

The [Ne II] 12.8 μm line of this BCG is also strong. Figure 2*b* plots the [Ne II] 12.8 μm luminosity against the infrared luminosity for a sample of nearby infrared-bright galaxies. As shown by Sturm et al. (2002), there is a good correlation between the two luminosities among the starburst and Seyfert galaxies, and the Z3146 BCG again stands out by having an exceptionally strong [Ne II] 12.8 μm line for its infrared luminosity (0.75%).

This overluminous [Ne II] emission line may also arise from a shock. However, the C-type shock invoked above to explain the H_2 level population cannot produce a substantial amount of the [Ne II] line because the shocked gas in a C-type shock is largely neutral and molecular. To produce the [Ne II] line, the shock must be a fast ($\gtrsim$50 km s^{-1}) J-type shock that can dissociate and ionize the shocked gas (e.g., Hollenbach & McKee 1989). The Z3146 BCG has an Hα velocity width of $\sim$600 km s^{-1} (Allen et al. 1992), so such a fast shock is plausible.

This probably means that various types of shocks may coexist in the Z3146 BCG. A similar conclusion was reached for NGC 6240 by Lutz et al. (2003) to account for the strong [O I] 63 μm line, which is also a sign of a J-type shock. Indeed, such a coexistence of the C- and J-type shocks is also seen in some Galactic outflow sources, in which both strong H_2 and [Ne II] lines are detected (e.g., Lefloch et al. 2003). Shock models can produce a wide range of [Ne III]/[Ne II] line ratios depending on various shock conditions, and therefore it is possible to produce the starburst-like [Ne III]/[Ne II] ratio with a strong shock (e.g., Binette et al. 1985; Hartigan et al. 1987). [Fe II] lines may also be used to constrain the shock conditions if their strengths are measured accurately.

With respect to the [Ne II] 12.8 μm line, the [S III] 18.7 μm line is abnormally weak ([S III]/[Ne II] < 0.05). Such a low [S III]/[Ne II] ratio is often seen with ultraluminous infrared galaxies, indicating that the gas-phase abundance of sulfur is significantly below solar (Genzel et al. 1998). Starburst galaxies also show this sulphur "deficiency," although the [S III]/[Ne II] ratios are less extreme, and this may suggest that the sulphur is depleted onto dust grains in high-metallicity star-forming systems (Verma et al. 2003).

5. CONCLUSIONS

We present the *Spitzer*/IRS mid-infrared spectrum of the infrared-luminous BCG in the X-ray–luminous cluster Z3146. The strong aromatic features indicate that the dominant source of the infrared luminosity is star formation. The most striking feature of the spectrum, however, is the exceptionally strong H_2 emission lines. To our knowledge, this BCG has the most luminous H_2 pure rotational emission lines and the most massive warm H_2 gas component ($\sim 10^{10}\ M_\odot$) known. Together with the large amount of cold H_2 detected previously ($\sim 10^{11}\ M_\odot$), this indicates that the Z3146 BCG contains disproportionately large amounts of both warm and cold H_2 gas for its infrared luminosity. Since the parent cluster Z3146 has an exceptionally large gas cooling rate in the core, these massive warm and cold H_2 components may be related to the intracluster gas cooling process.

We would like to thank G. Neugebauer and the anonymous referee for their comments, which improved the Letter. This work is based on observations made with the *Spitzer Space Telescope*, which is operated by the Jet Propulsion Laboratory, California Institute of Technology, under a contract with NASA (contract 1407). Support for this work was provided by NASA through an award issued by JPL/Caltech (contract 1255094).

REFERENCES

Allen, S. W., et al. 1992, MNRAS, 259, 67
Armus, L., et al. 2006, ApJ, 640, 204
Binette, L., Dopita, M. A., & Tuohy, I. R. 1985, ApJ, 297, 476
Böhringer, H., et al. 2000, ApJS, 129, 435
Burton, M. G. 1992, Australian J. Phys., 45, 463
Cowie, L. L., & Binney, J. 1977, ApJ, 215, 723
Crawford, C. S., Allen, S. W., Ebeling, H., Edge, A. C., & Fabian, A. C. 1999, MNRAS, 306, 857
Ebeling, H., Edge, A. C., Böhringer, H., Allen, S. W., Crawford, C. S., Fabian, A. C., Voges, W., & Huchra, J. P. 1998, MNRAS, 301, 881
Edge, A. C., Fabian, A. C., Allen, S. W., Crawford, C. S., White, D. A., Böhringer, H., & Voges, W. 1994, MNRAS, 270, L1
Edge, A. C., & Frayer, D. T. 2003, ApJ, 594, L13
Edge, A. C., Wilman, R. J., Johnstone, R. M., Crawford, C. S., Fabian, A. C., & Allen, S. W. 2002, MNRAS, 337, 49
Egami, E. 1998, in IAU Symp. 184, The Central Regions of the Galaxy and Galaxies, ed. Y. Sofue (Dordrecht: Kluwer), 95
Egami, E., et al. 2006, ApJ, 647, 922
Fabian, A. C., & Nulsen, P. E. J. 1977, MNRAS, 180, 479
Genzel, R., et al. 1998, ApJ, 498, 579
Goldader, J. D., Joseph, R. D., Doyon, R., & Sanders, D. B. 1997, ApJS, 108, 449
Hartigan, P., Raymond, J., & Hartmann, L. 1987, ApJ, 316, 323
Hicks, A. K., & Mushotzky, R. 2005, ApJ, 635, L9
Higdon, S. J. U., Arms, L., Higdon, J. L., Soifer, B. T., & Spoon, H. W. W. 2006, ApJ, 648, 323
Hollenbach, D., & McKee, C. F. 1989, ApJ, 342, 306
Houck, J. R., et al. 2004, ApJS, 154, 18
Jaffe, W., Bremer, M. N., & van der Werf, P. P. 2001, MNRAS, 324, 443
Kaufman, M. J., & Neufeld, D. A. 1996, ApJ, 456, 611
Le Bourlot, J., Pineau des Forêts, G., Flower, D. R., & Cabrit, S. 2002, MNRAS, 332, 985
Lefloch, B., Cernicharo, J., Cabrit, S., Noriega-Crespo, A., Moro-Martín, A., & Cesarsky, D. 2003, ApJ, 590, L41
Lutz, D., Sturm, E., Genzel, R., Spoon, H. W. W., Moorwood, A. F. M., Netzer, H., & Sternberg, A. 2003, A&A, 409, 867
Peeters, E., Spoon, H. W. W., & Tielens, A. G. G. M. 2004, ApJ, 613, 986
Rigopoulou, D., Kunze, D., Lutz, D., Genzel, R., & Moorwood, A. F. M. 2002, A&A, 389, 374
Sanders, D. B., Mazzarella, J. M., Kim, D.-C., Surace, J. A., & Soifer, B. T. 2003, AJ, 126, 1607
Sturm, E., Lutz, D., Verma, A., Netzer, H., Sternberg, A., Moorwood, A. F. M., Oliva, E., & Genzel, R. 2002, A&A, 393, 821
Sugai, H., Malkan, M. A., Ward, M. J., Davies, R. I., & McLean, I. S. 1997, ApJ, 481, 186
Thornley, M. D., Schreiber, N. M. F., Lutz, D., Genzel, R., Spoon, H. W. W., Kunze, D., & Sternberg, A. 2000, ApJ, 539, 641
van der Werf, P. P. 1996, in Cold Gas at High Redshift, ed. M. N. Bremer & N. Malcolm (Dordrecht: Kluwer), 37
Verma, A., Lutz, D., Sturm, E., Sternberg, A., Genzel, R., & Vacca, W. 2003, A&A, 403, 829
Weedman, D. W., et al. 2005, ApJ, 633, 706
Werner, M. W., et al. 2004, ApJS, 154, 1
Wilman, R. J., Edge, A. C., Johnstone, R. M., Fabian, A. C., Allen, S. W., & Crawford, C. S. 2002, MNRAS, 337, 63